Calculated electronic properties and reflectivity of tantalum*

J. F. Alward,† C. M. Perlov,† and C. Y. Fong†
Department of Physics, University of California, Davis, California 95616

C. Guha Sridhar
NASA Ames Research Center, Moffett Field, California 94035

(Received 7 June 1976)

A nonrelativistic band structure of the bcc transition metal tantalum has been calculated by an iterative empirical-pseudopotential method. Main peak locations in the density of occupied states agree to better than 0.3 eV with the results of two earlier augmented-plane-wave calculations, while the main peak in the density of unoccupied states is more than 1 eV lower than the main peak in either of the previous results. In the context of direct transitions, the constant-matrix-element approximation is shown to be generally valid for Ta. In addition, reflectivity spectra based on the $\vec{k}$-dependent, direct transition model, and the nondirect transition model have been calculated, and each spectrum is in comparably good agreement with the data of Weaver, Lynch, and Olson. *Modulated* reflectivity spectra have also been calculated according to both models, and the results suggest that measurements of this quantity might help to determine which of the two types of transitions—direct or nondirect—predominates in Ta. Finally, the calculated Fermi surface agrees well with the data of Halloran *et al.*

I. INTRODUCTION

The usefulness of electronic-energy-band structures in interpreting the physical properties of solids is well known. But in recent years, much work has been done in the opposite direction: using experimental data to determine a solid's energy-band structure via the empirical-pseudopotential method.[1] In this regard, optical-reflectivity, photoemission, and Fermi-surface data are among the more valuable types of data used in fitting energy-band structures. Of course, the ultimate goal in such studies is not simply that of obtaining an energy-band structure which is consistent with these data, but rather it is to use the derived band structure to help explain or predict other important properties, such as superconductivity and bonding characteristics.

Group-V (V, Nb, Ta) transition metals have many properties of practical interest, such as hardness and high-temperature superconductivity.[2] Extensive experimental investigations of the electronic properties of these elements had been stalled in the past because of the lack of good single crystals, but their recent availability has led to measurements of their optical[3] and Fermi-surface[4,5] properties. In part because of the existence of these data, and also because of the need to better understand the physical properties of these important superconducting transition metals, we have begun a theoretical investigation of the electronic properties of the group-V elements. Our study begins with tantalum.

Tantalum's transition temperature ($T_c = 4.48$ K) is one of the highest for a nonalloy, and it is one of the hardest of all the transition-metal elements. There is thus considerable practical value in a theoretical study of its electronic properties. An additional value of the present Ta study lies in the possible use of its pseudopotential, together with that for Se,[1] to calculate the electronic properties of the layer compounds $1T$-$TaSe_2$ and $2H$-$TaSe_2$, which display the interesting charge-density-wave properties recently observed by Wilson *et al.*[6]

Since the electronic wave functions of the energy states near the Fermi surface can be used to calculate electron-phonon interactions and electronic charge distributions, an accurate determination of these wave functions is essential if such calculations are to be undertaken. The goal of the present work is to obtain these wave functions via an empirical-pseudopotential band-structure calculation.

Before detailing our methods of calculation, we will first discuss a recent controversy regarding the relative merits of the *direct* and *nondirect* transition models. In the direct transition model, the electron's crystal momentum, $\vec{k}$, is conserved in the excitation process. Crystal momentum, however, need not be conserved in the nondirect model. Analysis of photoemission data for noble and transition metals prompted Spicer and coworkers[7] to suggest that $\vec{k}$ conservation is not an important selection rule, especially for those transitions involving d states. More recent work, however, has shown that it is possible to explain copper photoemission data in terms of direct

transitions.[8]

On the other hand, considerable support for the nondirect model has been recently provided by Steel,[9] who showed that observed structure in the absorption coefficient of V, Cr, and Mn can be successfully explained by this model. To confuse matters further, Koelling *et al.*[10] have calculated the optical properties of Mo using both the direct (in the *constant*-matrix-element approximation) and the nondirect models. While there are some distinct disimilarities between the results of the two models, both still compare favorably with the data. To date, there is thus widespread disagreement about the relative importance of direct and nondirect transitions in the transition metals. While the intent of the present work is not to resolve the controversy, our results will nevertheless suggest that future experimental determinations of modulated reflectivity spectra might help determine which of the two types of transitions predominate in Ta.

A tantalum energy-band structure is obtained in the present study by using the empirical pseudopotential method to fit the energy bands *at* the Fermi level to the data of Halloran *et al.*[4] Since agreement with Fermi-surface data is not a sensitive test of the energy bands *away* from the Fermi level, we have also simultaneously fitted our band structure to the data of Weaver, Lynch, and Olson.[3] It is agreement with *both* sets of data which provides the more strict test of the accuracy of the energy bands and wave functions. But, in light of the obvious uncertainties regarding the relative importance of direct and nondirect transitions, we have calculated the reflectivity according to both models. For the direct model, the $\vec{k}$-dependent dipole transition matrix elements are used. For transition metals, as far as we know, the present work is the first comparison of the nondirect model with the $\vec{k}$-dependent direct model.

There have been two earlier determinations of tantalum's energy-band structure. The first, a relativistic, augmented-plane-wave (RAPW) calculation by Mattheiss,[11] is in good agreement with the Fermi-surface measurements of Ref. 4. The RAPW energy bands *in the immediate vicinity of the Fermi level*, therefore, may be assumed to be very accurate—to better than about 0.2 eV. But, neither reflectivity nor photoemission data existed at that time, so these quantities—which might have confirmed the locations of the bands *away* from the Fermi level—were not calculated. Questions regarding the accuracy of these bands thus remain unanswered. The same may be said of another Ta APW band-structure calculation by Petroff and Viswanathan.[12] While they did not calculate the Ta Fermi surface, they did evaluate the dipole transition matrix elements and calculate the energy distribution function for photoemission. However, an evaluation of their results must await future Ta photoemission data.

II. PRESENT METHODS OF CALCULATION

Detailed discussion of the empirical pseudopotential method is in the literature.[1] We have not included the spin-orbit interaction. In this section we will just discuss a new iteration scheme we have developed—a scheme which permits a rapid determination of a near-optimum pseudopotential.

Since the diagonalization of large secular determinants in pseudopotential calculations involves large amounts of computer time, it is important to use very effective means in searching for an empirical pseudopotential which provides good agreement with all experimental data. In the past, inspection[1] and nonlinear optimization schemes[13] have been used. While these schemes have had great success in calculations of band structures wherein single $\vec{k}$ points (critical points) play a dominant role in the optical behavior, there are nevertheless many elements which display so-called "volume effects." In these solids, the main peaks in the reflectivity arise—not from critical points—but from large regions throughout the Brillouin zone. In order to deal effectively with these volume effects, the following scheme was developed.

1. *Choose a starting pseudopotential.* Since no previous Ta pseudopotential has been given in the literature, the starting pseudopotential in the present case is taken to be that used by Fong and Cohen[14] in their empirical-pseudopotential-method (EPM) band-structure calculation of niobium, the element just above tantalum in Group V of the periodic table. In that work, as in the present, eight parameters are used to characterize the pseudopotential. Four of these parameters correspond to the coefficients [form factors, $V(|\vec{G}|^2)$] of a truncated Fourier expansion of the local pseudopotential, two correspond to the depth and width of the nonlocal square d well, and two others, α and κ, are involved in the d-state damping factor $e^{-\eta}$, where $\eta = \alpha[(|\vec{k}+\vec{G}| - \kappa)/2k_F]^2$, $\vec{k}$ is the wave vector, $\vec{G}$ is a reciprocal-lattice vector, and k_F is the Fermi momentum. The off-diagonal nonlocal matrix elements are multiplied by the damping factor to improve the convergence of the d-like wave functions.

2. *Calculate the energy-band structure.* Energy convergence to within 0.1 eV is obtained with about 110 plane waves, corresponding to $|\vec{k}+\vec{G}|^2 \leq 14.1(2\pi/a)^2$, where $\vec{k}$ is one of 91 uniformly dis-

tributed mesh points in the irreducible part of the Brillouin zone, $\vec{G}$ is a reciprocal-lattice vector, and $a = 3.30$ Å is the lattice constant.[15] The Löwdin perturbation scheme[16] is not used.

3. *Calculate the density of states.* The distribution of energy states is obtained from about 10 000 linear interpolations in the 91-point irreducible zone mesh.

4. *Determine the Fermi energy and the shape of the Fermi surface.* The Fermi energy is determined by integrating the density of states to five electrons, the valency of Ta. Then a linear interpolation in the 91-point mesh is used to map out the Fermi-energy contours.

5. *Calculate the imaginary part of the dielectric function,* $\epsilon_2(\omega)$. The method used for the direct transitions model is described by Saslow *et al.*[17] In the present iterative procedure, only the direct transition model is used. Once a final band structure is determined, ϵ_2 and the reflectivity are determined according to the nondirect model. In this model,

$$\epsilon_2 \sim \frac{1}{\omega^2} \int N(E)\, N(E+\hbar\omega)\, dE,$$

where $N(E)$ and $N(E+\hbar\omega)$ are the densities of states at the valence- and conduction-band energies, respectively. For both models, the total ϵ_2 is taken to be the sum of the interband and free-electron parts.[18]

6. *Calculate the reflectivity.* A Kramers-Krönig transformation[19] of the total $\epsilon_2(\omega)$ is used to calculate the real part of the dielectric function, $\epsilon_1(\omega)$. From these two quantities, the reflectivity, $R(\omega)$, is calculated on the assumption of normal-incidence photons.[20]

7. *Compare Fermi surface and reflectivity with experiment.* Specific areas of agreement sought for the Fermi surface are the cross-sectional areas of the hole ellipsoids at the N symmetry point, and the minimum arm diameter of the jungle gym. The comparison of the calculated reflectivity with data is more subjective. Evaluation of the extent of agreement is guided by considerations of general shape, magnitude, and locations of prominent structure below 6 eV. When comparisons with the data—for both the Fermi surface and the reflectivity are unsatisfactory, another set of pseudopotential parameters is chosen according to steps 8 and 9.

8. *Vary the pseudopotential.* Each of the eight pseudopotential parameters can, in principle, assume any one of a continuous, but limited range, of new values. An infinite number of possible new sets of pseudopotential parameters are therefore available. But, of course, as a practical matter, we must restrict the scope of the search. Instead of permitting variations of all eight of the parameters, the parameters relating to the d-state damping factor and the width of the d well retain their starting values, and only the four form factors and the depth of the d well are allowed to vary. Changes are not made continuously, but are instead taken to be either zero, or plus, or minus some small, but fixed amount (~0.01 Ry). The search is thus limited to five parameters, each of which may independently assume any one of three different values. There are then $3^5 = 243$ new pseudopotentials to test. First-order perturbation theory is used to determine new, approximate energy-band structures for each of these pseudopotentials. Initially, though, only the energies at the symmetry points are calculated to see whether those states which lie within 2–3 eV of the Fermi level are in severe disagreement with the earlier *a priori* calculations.[11,12] For the EPM energy states more than about 3 eV above the Fermi level, we do not demand similarity with the *a priori* results. Indeed, the essence of the EPM is that the Fourier expansion of the pseudopotential may be truncated to exclude all but the long-wavelength (low-energy) terms, so the EPM bands lying within 2–3 eV of the Fermi surface may be regarded as relatively accurate (to within 0.1 eV), while the higher-energy states may be inaccurate. Since the goal of the present study is to obtain accurate wave functions for only the energy states within 2–3 eV of the Fermi level, the inherent uncertainty in the higher-energy states makes no difference in the present calculation. If the perturbed energies do not satisfy the *a priori* constraints, the associated pseudopotential is discarded. However, a full 91-point perturbed band structure[21] is calculated for each pseudopotential that does satisfy these constraints. Each of these approximate band structures is then used to calculate an approximate Fermi surface and reflectivity according to steps 3–6.

9. *Select the best pseudopotential.* Determine which of the above 243 pseudopotentials provides the best agreement with the data, and use it as the new starting pseudopotential in step 2.

The above iterative procedure continues until the comparison with experiment is optimum. Steps 2–9 are all included in a single computer program. The results reported in Sec. III were obtained after five iterations.

III. RESULTS

A. Band structure

The final pseudopotential parameters are compared with the starting values in Table I. Also given is the free-electron parameter $\gamma = m^*/n$,[18]

TABLE I. Comparison between the present tantalum EPM parameters and the EPM parameters for niobium from Ref. 14.

EPM Parameters[a]	Present Results (Ry)	Ref. 14 (Ry)
$V(2)$	−0.041	−0.041
$V(4)$	0.100	−0.020
$V(6)$	0.071	−0.009
$V(8)$	0.150	0.070
Depth of d well	−3.483	−3.884
α	0.206	0.206
κ	$1.668(2\pi/a)$	$1.668(2\pi/a)$
γ	1.1×10^{-49} g cm^3	

[a]Arguments of the form factors $V(|G|^2)$ are given in units of $(2\pi/a)^2$, where $a=3.30$ Å.

this parameter is not one of those varied during the iteration scheme, but was adjusted to its present value after the final values for the other parameters were obtained. Note that all but the first of these parameters are considerably higher than the starting values. The average difference in the form factors is 0.07 Ry, while the nonlocal d well of Ref. 14 is 0.401 Ry deeper. The large difference in the depths of the d wells is due to the relative insensitivity of the d-state energies to changes in the depth. The relatively large difference between the starting and final pseudopotential parameters illustrates the power of the present iterative technique.

The calculated energy bands are shown in Fig. 1. The standard notation is used to label the symmetry points and lines.[22] Generally, the occupied bands are in reasonable agreement with the APW bands.[11,12] In the unoccupied states, however, there are apparent differences. These differences are discussed below.

The Δ_1 band intersecting both $\Delta_{2'}$ and Δ_5 provides one of the more striking contrasts between the earlier APW results and the present EPM calculation. Near its endpoints, the present Δ_1 band lies above $\Delta_{2'}$ and Δ_5, but dips below both of these bands at a point about $\frac{2}{3}$ of the way from Γ_{12} to H_1. No dip is evident in the work of Ref. 12, where the Δ_1 band has a free-electron-like shape and lies well above $\Delta_{2'}$ and Δ_5. The dip is obvious in Ref. 11, but it is not as strong as in the present case. A second significant difference is found at the N symmetry point, where the present N_4 ($5d$) state is located only 1.6 eV above the Fermi level, but in Ref. 11, N_4 is at 4.4 eV, and at 4.1 eV in Ref. 12. Another important difference is at the P symmetry point, where P_1 is very low compared to the APW results. It is 4.7 eV, and 8.0 eV lower than the P_1 state in Refs. 11 and 12, respectively. A final difference is found about 7 eV above the Fermi level, at the H symmetry point. Here, the ordering $(H_1$-$H_{15})$ is the opposite of that obtained in Refs. 11 and 12. In addition, both of these states are quite low compared to these earlier works. The present features are probably artifacts of the EPM. However, these states are too high to influence the calculation of the reflectivity below 6 eV.

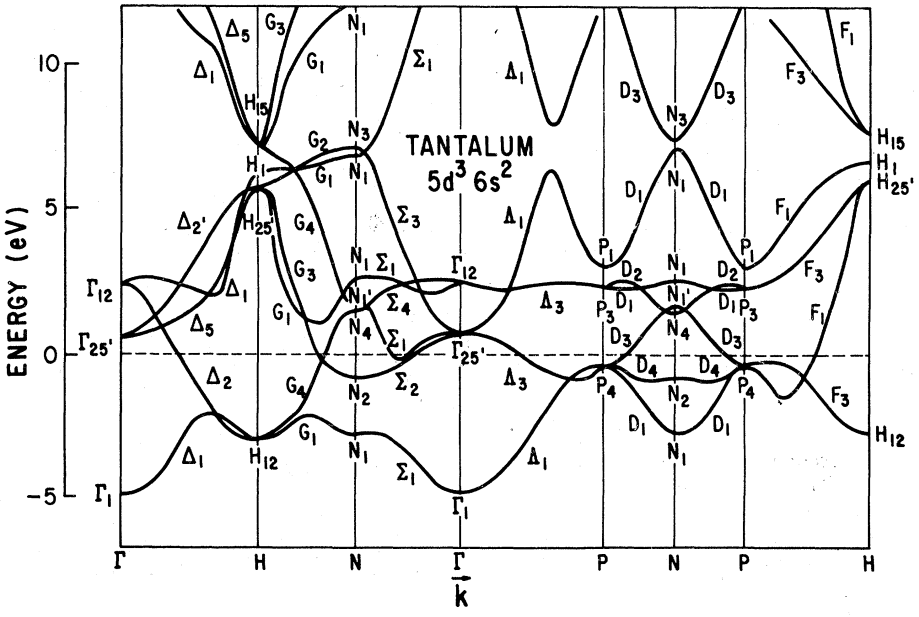

FIG. 1. Empirical pseudopotential band structure of tantalum. Fermi level is indicated by the broken horizontal line, taken as the zero of energy.

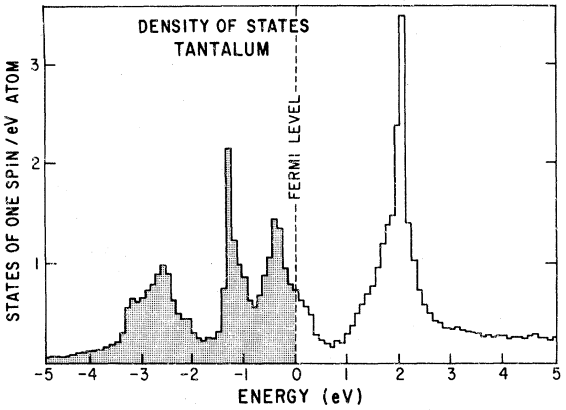

FIG. 2. Electronic density of states of tantalum. Shaded area represents the occupied region.

B. Density of states

The calculated density of states, $N(E)$, is given in Fig. 2 as a histogram of 0.1 eV resolution. A broken vertical line indicates the Fermi level; the estimated uncertainty in its position is 0.05 eV. In the present work, the main peak above the Fermi level is located at 2.0 eV, while the main peak in Ref. 11 is at 4.5 eV, and at 4.1 eV in Ref. 12. These differences are closely related to the band-structure differences discussed in Sec. III A. Below the Fermi level, there are three main peaks, located at -0.3, -1.2, and -2.5 eV. In Ref. 11, the main peaks below the Fermi level are at -0.3, -1.5, and -2.6 eV, and at 0.0, -1.5, and -2.7 eV in Ref. 12. The present density of occupied energy states thus agrees to within -0.3 eV with both APW calculations. Finally, the density of states at the Fermi level, $N(E_F)$, is 0.78 states of one spin/(eV atom). This result is in excellent agreement with the value obtained by McMillan,[23] who used a strong coupling formulation to derive the value 0.77 from the experimental values of the superconducting transition temperature and the electronic specific-heat capacity. In contrast, the calculated values of $N(E_F)$ from Refs. 11 and 12 are 0.65 and 0.61.

C. Imaginary part of the dielectric function

Theoretical spectra of the imaginary part of the interband dielectric function, $\epsilon_2(\omega)$, based on the direct transition model, have been calculated, first, for $\vec{k}$-dependent dipole-transition pseudo-matrix elements,[24] shown in Fig. 3 as the solid curve. A calculation of $\epsilon_2(\omega)$ based on constant matrix elements is shown as the dashed curve. The qualitative features of these two direct transition curves are very similar. There is a one-to-one correspondence of the individual structures, and the relative magnitudes and shapes of the curves show good agreement. Enhancement, relative to the peaks at 2.6 and 4.3 eV, of all the other structures in the constant-matrix-element curve is the main effect of including the matrix elements. The similarity of these two curves strongly suggests that the assumption of constant matrix elements—based on the direct transition model in Ta—is generally valid. It seems probable that the assumption is also valid for tantalum's neighbors on the periodic table—V, Nb, Mo, and W. Such an assumption was made by Pickett and Allen,[25] who used the APW band structures of Nb,[11] and Mo,[12] to calculate the imaginary part of the dielectric function, ϵ_2. The agreement with the experimental data of Ref. 3 is fairly good.

The results of the present calculation of ϵ_2, based on the nondirect transition model, are shown as the chain curve in Fig. 3. While this curve is in qualitative agreement with the others, there are nevertheless four main points of dissimilarity. First, and most obvious, is the difference below 1 eV. An abrupt rise to a maximum at 0.2 eV, and an equally rapid fall to a minimum at 0.9 eV are dominant features of the direct transition model. The strong peak at 0.2 eV is associated with direct transitions at off-symmetry points between second and third bands very close to the

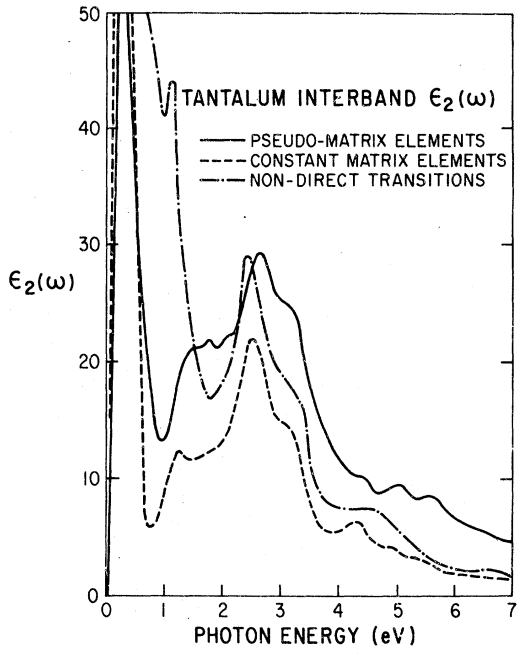

FIG. 3. Imaginary part of the interband dielectric function, $\epsilon_2(\omega)$, calculated using pseudomatrix elements (solid curve), constant matrix elements (dashed curve), and for nondirect transition (chain curve).

Fermi level. These band pairs cannot be seen in Fig. 1, but they are derived from the relatively flat, doubly degenerate Λ_3 band, which splits at $\vec{k}$ points away from the symmetry line. Even though the dipole transition probabilities for these transitions are about ten times smaller than those contributing to the other peaks, this peak is still very strong because of the relatively large joint density of states associated with the two almost parallel band pairs—one just above, and the other just below the Fermi level. The peak is also greatly enhanced by the $1/\omega^2$ weighting factor which occurs in the integral expression for $\epsilon_2(\omega)$.[17] In the nondirect curve, there is no peak in the low-energy portion of the spectrum, which goes off scale at 0.7 eV and rises monotonically. Secondly, the nondirect model shows no structure between 1 and 2 eV, while there is a definite shoulder in this portion of the direct transition curve. About 40% of the strength of this shoulder comes from transitions between the second and third bands (2–3 transitions) at $\vec{k}$ points on and just above the central region of the ΓNH symmetry plane; another 40% arises from 3–4 transitions inside a roughly spherical region of radius $|\vec{k}| \sim \frac{1}{4}(2\pi/a)$, centered near $\vec{k} = (\frac{1}{2}, 0, 0)$.

A third significant difference is the location of the main peak. Transitions from the high density of states at -0.4 eV, to the high density of states at 2.0 eV are responsible for the main nondirect peak at 2.4 eV. However, the direct model predicts a strong peak at 2.7 eV, whose strength is due mainly to 1–3 (31%) and 2–4 (31%) transitions at $\vec{k}$ points throughout the central region of the Brillouin zone. Finally, above 4 eV in the nondirect curve, there is a smooth broad peak near 4.6 eV which arises from transitions between the high densities of states at -2.6 and 2.0 eV. On the other hand, a succession of several small structures above 4 eV characterizes the direct transition curve. Aside from these differences, the direct and nondirect transition models predict interband ϵ_2 spectra which are roughly similar above 1.5 eV, and even these differences below 1.5 eV are almost neutralized by the strong free-electron contribution in Fig. 4.

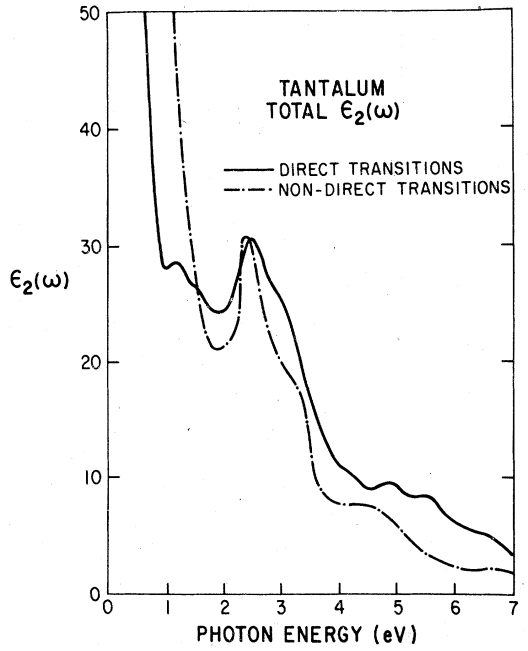

FIG. 4. Sum of the interband ϵ_2 and the free-electron ϵ_2. Solid curve corresponds to the direct transition model, and the chain curve is the nondirect result.

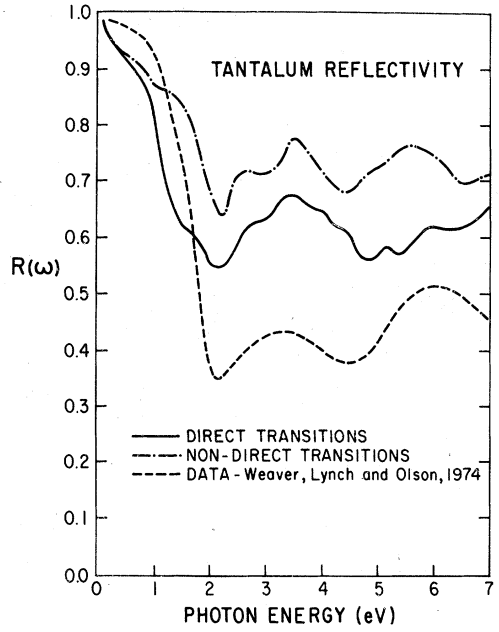

FIG. 5. Tantalum reflectivity spectra. Solid curve is based on the direct transition model (with $\vec{k}$-dependent dipole matrix elements), the chain curve is based on the nondirect model, and the broken curve is the data of Ref. 3.

D. Reflectivity

Theoretical reflectivity spectra based on the direct and nondirect transition models are shown in Fig. 5 as the solid and chain curves, respectively. Both theoretical spectra have roughly the same shape as the data, shown as the dashed curve. The direct transitions model predicts a spectra which is 0.2–0.3 higher in reflectivity than the data. This discrepancy may be in part due to the relative (~5%) inaccuracies involved in using the pseudo-wave-functions to calculate

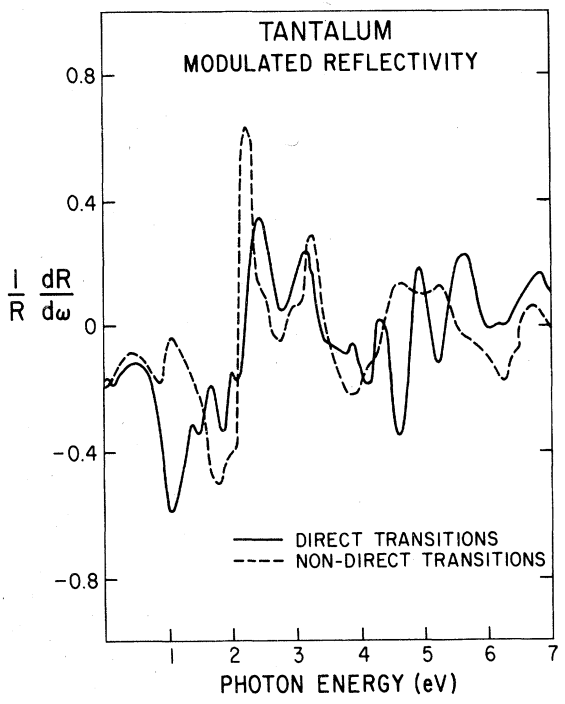

FIG. 6. Calculations of the modulated reflectivity spectra, based on the direct transition model (solid curve), and the nondirect transition model (broken curve).

the dipole-transition matrix elements.[24] Magnitude differences between the data and the nondirect results are of no significance, since constant matrix elements are assumed. The value of the constant is somewhat arbitrarily chosen to be that which permits the direct and nondirect curves to be of comparable magnitude. Both models predict a broad multistructured peak, located above the peak at 3.4 eV in the data. The shape of the direct transitions peak is in generally better agreement with the data. However, the prominent peak at 6 eV in the data more clearly corresponds to the peak at 5.7 eV in the nondirect curve. On the whole, then, either curve may be regarded favorably, based on the agreement of each with the data. Given the inherent and unavoidable uncertainty regarding the true nature of the optical excitation process in these transition metals, the present results should be regarded as satisfactory. Any effort to make further slight improvements would probably be of little value, since one could always argue that the ambiguous nature of the transitions would make such fine tuning meaningless.

The rough, qualitative similarity of the results of the direct and nondirect reflectivity calculations is a feature which the authors have found to be invariant for transition-metal band structures. Thus, reflectivity measurements will probably not be sufficient to distinguish between the two types of transitions in these metals, because the EPM can be used to fit the reflectivity data comparably well with either model.

Modulated reflectivity measurements, however, may be the key to resolving the present controversy. We have used both models to calculate the modulated reflectivity for Ta, and the results, shown in Fig. 6, show a great many important qualitative differences, especially below 2 eV and above 4 eV, where the structure in the direct model is much sharper than in the direct model. The differences between the two models are great enough to suggest that it would probably be extremely difficult to obtain a comparably good fit to modulated reflectivity data, using both models. Thus, future measurement of the modulated reflectivity of Ta could be used, together with Fermi-surface and reflectivity data, to fit an EPM band structure of Ta, and then, perhaps, finally resolve which of the two types of transitions predominate in Ta.

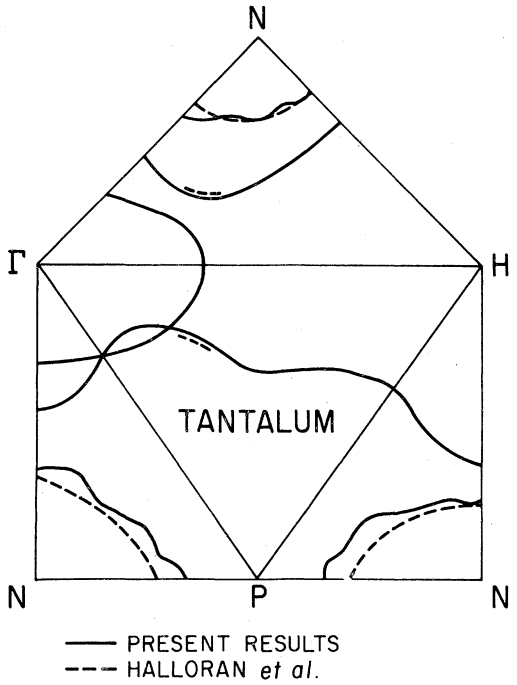

FIG. 7. Cross sections of the Ta Fermi surface, showing the distorted hole ellipsoids at N, the octahedral hole surface at Γ, and the jungle-gym arm along $\overline{\Gamma H}$. Solid curves are the present results and the broken curves correspond to the data of Ref. 4.

TABLE II. Comparison of the present principal energy gaps with the energy gaps of Refs. 11 and 12.

	$\Gamma_{12}-\Gamma_{25'}$	$E_F-\Gamma_1$	$\Gamma_{25'}-E_F$	E_F-H_{12}	$N_{1'}-\Gamma_1$	$N_{1'}-E_F$	E_F-P_4	P_3-E_F	P_1-E_F
					(eV)				
Present results	1.8	5.0	0.6	3.0	6.7	1.9	0.5	2.1	3.0
Ref. 11	2.7	8.6	0.8	3.9	8.8	1.5	1.1	4.6	7.4
Ref. 12	2.7	5.5	0.5	4.1	8.1	2.6	1.0	4.2	10.7

E. Fermi surface

Central cross sections of the Ta Fermi surface are shown in Fig. 7. Calculated Fermi-energy contours are shown as the solid curves. The broken contours were derived from the data of Ref. 4. We have assumed that the areas reported in that work correspond to cross sections of perfect ellipsoids. It is known,[4] however, that the experimentally observed ellipsoids bulge out along the $N\Gamma$ symmetry line. The present ellipsoids have a "wobbly" appearance, and the calculated areas for these ellipsoids agree with the data to within 10%. Precise values for the area have not been calculated because of the relative crudeness of the present interpolation scheme, and because the calculation would involve the comparatively inaccurate method of adding up grid squares. Also shown is the cross section of the so-called jungle gym. The dashed portion corresponds to the observed minimum diameter of the arm. The present contours are similar to the results of Ref. 11. In that work, however, the hole ellipsoids have very little distortion, and, in the ΓHP plane, the jungle-gym arm does not intersect the octahedral hole surface, as in the present case. But their jungle-gym arm in the ΓNH plane apparently does intersect this surface, while the arm and octahedral contours are well-separated in our work. Finally, referring back to Fig. 1, the minimum of the Σ_1 band nearest the Fermi level is just 0.2 eV below the surface. This characteristic is important, since the ellipsoids at the N symmetry point would open up along the Σ directions and form necks joining the ellipsoids to the jungle gym if Σ_1 were to fail to dip below E_F. Because the minimum is quite near E_F, it is quite clear that even very small changes in the pseudopotential could have a significant effect on the shape of the Fermi surface.

IV. SUMMARY

An effective new scheme to determine the empirical pseudopotential has been used to calculate a tantalum energy-band structure. The present occupied density of states is in qualitative agreement with earlier APW calculations.[11,12] There is significant disagreement, though, above the Fermi level. However, the present calculated value of the density of states at the Fermi levels is in excellent agreement with the value obtained by McMillan.[23]

Within the context of the direct transition model, the constant-matrix-element approximation has been shown to be generally valid for Ta. In addition, the reflectivity of Ta has been calculated using both the nondirect- and the $\vec{k}$-dependent direct transition models, and both spectra are in comparably good agreement with the data of Ref. 3. Because of the similarity of the two theoretical reflectivity spectra, it is clear that Fermi-surface and reflectivity data alone will not be sufficient to determine which of the two types of transitions predominates in Ta. The large differences between the *modulated* reflectivity spectra, calculated according to both the nondirect and direct transition models, however, suggest that measurements of this quantity might be used by the EPM to discriminate between these types of transitions.

Cross sections of the tantalum Fermi surface have been mapped out, and they are in agreement with the data of Ref. 4. Furthermore, except for minor differences, the present Fermi surface is in fair agreement with the RAPW Fermi surface of Ref. 11.

In conclusion, the fair agreement with the reflectivity data below 7 eV—for both direct and nondirect transition models—indicates that the *relative* locations of the energy bands are accurate to within 0.5 eV, and the agreement with the Fermi-surface data has confirmed, to within about 0.2 eV, the accuracy of the *absolute* locations of the energy bands *at* the Fermi level. We believe that the present results are sufficiently accurate to encourage further calculations of electron-phonon interactions and charge distribution in Ta.

ACKNOWLEDGMENTS

We are indebted to Dr. J. H. Weaver, Synchrotron Radiation Center, University of Wisconsin-Stoughton, who provided a complete listing of the Ta reflectivity data. We also wish to acknowledge the cooperation and assistance provided by Dr. E. E. Whiting, NASA Ames Research Center, Moffett Field, California.

*Funds for part of this study have been provided by NASA-Ames Research Center, Moffett Field, California, under interchange NCA2-OR180-502.
†Supported in part by the U. S. AFOSR (AFSC) under Grant No. AFOSR-72-2353.

[1]M. L. Cohen and V. Heine, *Solid State Physics*, edited by F. Seitz and D. Turnbull (Academic, New York, 1970), Vol. 24.
[2]B. W. Roberts, *Progress in Cryogenics* (Heywood, London, 1964); F. Heininger, E. Bucher, and J. Muller, Phys. Kondens. Mater. 5, 243 (1966).
[3]J. H. Weaver, D. W. Lynch, and C. G. Olson, Phys. Rev. B 10, 501 (1974).
[4]M. H. Halloran, J. H. Condon, J. E. Graebner, J. E. Kunzler, and F. S. L. Hsu, Phys. Rev. B 1, 366 (1970).
[5]R. A. Phillips, Phys. Lett. A 36, 361 (1971); Robert D. Parker and Michael H. Halloran, Phys. Rev. B 9, 4130 (1970).
[6]J. A. Wilson, F. J. DiSalvo, and S. Mahajan, Phys. Rev. Lett. 32, 882 (1974).
[7]C. N. Berglund and W. E. Spicer, Phys. Rev. 136, A1030 (1964); A. J. Blodgett and W. E. Spicer, *ibid.* 146, 390 (1966); W. F. Krolikowski and W. E. Spicer, *ibid.* B 1, 478 (1970).
[8]N. V. Smith and W. E. Spicer, Opt. Commun. 1, 157 (1969); P. O. Nilsson, C. Norris, and L. Wallden, Phys. Kondens. Mater. 11, 220 (1970).
[9]M. R. Steel, J. Phys. F 4, 783 (1974).
[10]D. D. Koelling, F. M. Mueller, and B. W. Veal, Phys. Rev. B 10, 1290 (1974).
[11]L. F. Mattheiss, Phys. Rev. B 1, 373 (1970).
[12]Irene Petroff and C. R. Viswanathan, Phys. Rev. B 4, 799 (1971).
[13]John P. Walter and M. L. Cohen, Phys. Rev. 183, 763 (1969).
[14]C. Y. Fong and M. L. Cohen, Phys. Lett. A 44, 375 (1973).
[15]R. W. G. Wyckoff, *Crystal Structure*, 2nd ed. (Interscience, New York, 1963), Vol. 1, p. 16.
[16]P. Löwdin, J. Chem. Phys. 19, 1396 (1951).
[17]W. M. Saslow, T. K. Bergstresser, C. Y. Fong, M. L. Cohen, and D. Brust, Solid State Commun. 5, 667 (1967).
[18]J. F. Alward, C. Y. Fong, M. El-Batanouny, and F. Wooten, Phys. Rev. B 12, 1105 (1975). In this work, the free-electron contribution is shown to be fully determined by the experimental value of the electrical conductivity, and one adjustable parameter $\gamma = m^*/n$, where m^* is the effective mass of the electron and n is the effective concentration of free electrons.
[19]F. Wooten, *Optical Properties of Solids* (Academic, New York, 1972), p. 179.
[20]J. M. Ziman, *Principles of the Theory of Solids* (Cambridge U.P., London, 1972), p. 258.
[21]An approximate (to within 0.1 eV) calculation of the full energy-band structure based on perturbation theory uses about 100 times less computer time than an exact calculation based on a diagonalization of a 110×110 matrix.
[22]L. P. Bouckaert, R. Smoluchowski, and E. Wigner, Phys. Rev. 50, 58 (1936).
[23]W. L. McMillan, Phys. Rev. 167, 331 (1968).
[24]It is important to note that the pseudo-wave-functions are, of course, by definition, not the true wave functions—which are orthogonal to any of the core states. However, the wave functions of interest to us are those which correspond to electrons which are least tightly bound to the individual nuclei—they are comparatively free electrons, and are thus adequately described by the pseudo wave functions. The authors have calculated the dipole-transition matrix elements with wave functions obtained from an orthogonalization of the pseudo wave functions to the core states of Ta. We have found that there is less than 5% difference in these values, compared to a calculation using the pseudo wave functions.
[25]Warren E. Pickett and Phillip B. Allen, Phys. Rev. B 10, 3599 (1975).